

Articles

Aragonite–Hydroxyapatite Conversion in Gastropod (Abalone) Nacre

Charlotte M. Zaremba,[†] Daniel E. Morse,[§] Stephen Mann,[‡] Paul K. Hansma,[#] and Galen D. Stucky^{*,†,||}

Department of Chemistry, Marine Biotechnology Center and Department of Molecular, Cellular, and Developmental Biology, Department of Physics, and Materials Department, University of California, Santa Barbara, California 93106, and School of Chemistry, University of Bath, Bath BA2 7AY, United Kingdom

Received December 2, 1997. Revised Manuscript Received September 18, 1998

From studies of geological and coral skeleton aragonite, it was previously proposed that aragonite converts hydrothermally to hydroxyapatite (HA) in phosphate solution by a solid-state topotactic ion-exchange reaction in which the HA retains the orientation of the original aragonite. The present investigation of this reaction in gastropod shell nacre suggests instead that conversion for this biomineral proceeds via dissolution-recrystallization, with the preferred orientation of the product determined by the flux direction of the solution through the material. Conversions of various CaCO_3 biominerals in aqueous $(\text{NH}_4)_2\text{HPO}_4$ at 140–260 °C show that for gastropod nacre alone, sample form and internal ultrastructure are largely preserved and a unique preferred orientation arises: with reaction time, HA nanocrystallites are increasingly oriented with their *c*-axes perpendicular to the *c*-axis of the original aragonite. In contrast, other CaCO_3 biominerals either disintegrate to HA powder or contain HA crystallites with random orientation or the orientation of the original aragonite. We suggest that the organic matrix of gastropod nacre channels the reaction solution through the material vertically between stacks of aragonite tablets so that sample form and internal ultrastructure are preserved and the HA predominantly adopts a perpendicular *c*-axis orientation. Other properties of HA-converted gastropod nacre are also discussed.

Introduction

Crystallization of hydroxyapatite (HA), $\text{Ca}_5(\text{OH})(\text{PO}_4)_3$, and its congeners is the subject of extensive research due to the biological importance of this inorganic phase. Most preparations involve either hydrothermal synthesis or aqueous precipitation followed by aging.^{1–3} However, another route is replacement of the calcite or aragonite polymorph of CaCO_3 in phosphate solution. This reaction is well-known to geologists^{4–8}

and achieved prominence in 1974, when the aragonite of *Porites* coral skeleton was converted hydrothermally to HA with preservation of its 0.2-mm-pore architecture.^{9,10} The product is an effective, commercially available bone implant material because it contains an interconnected network of channels appropriate for bone cell ingrowth that is comprised of HA, a biomaterial that stimulates bone growth without immune response complications.^{11–13}

The aragonite–HA conversion was characterized as a topotactic ion exchange reaction because HA (hexagonal, $a = 9.43 \text{ \AA}$, $c = 6.88 \text{ \AA}$, $\gamma = 120^\circ$) and aragonite when described as pseudo-hexagonal ($a = 9.39 \text{ \AA}$, $c = 5.74 \text{ \AA}$, $\gamma = 117^\circ$) have similar lattice parameters, ionic positions, and ionic contents.¹⁴ Moreover, when conversion is conducted with *ab*-face slices of geological aragonite, sample form is preserved and the *c*-axes of

* To whom correspondence should be addressed.

[†] Department of Chemistry, University of California.

[§] Marine Biotechnology Center and Department of Molecular, Cellular, and Developmental Biology, University of California.

[‡] University of Bath.

[#] Department of Physics, University of California.

^{||} Materials Department, University of California.

(1) Ishikawa, T.; Wakamura, M.; Kawase, T.; Kondo, S. *Langmuir* **1991**, *7*, 596.

(2) Arends, J.; Christoffersen, J.; Christoffersen, M. R.; Eckert, H.; Fowler, B. O.; Heughebaert, J. C.; Nancollas, G. H.; Yesinowski, J. P.; Zawacki, S. J. *J. Cryst. Growth* **1987**, *84*, 515.

(3) Lerner, E.; Azoury, R.; Sarig, S. *J. Cryst. Growth* **1989**, *97*, 725.

(4) Narasaraju, T. S. B.; Phebe, D. E. *J. Mater. Sci.* **1996**, *31*, 1.

(5) Ames, L. L., Jr. *Econ. Geol.* **1959**, *54*, 829.

(6) Gulbrandsen, R. A. *Econ. Geol.* **1969**, *64*, 365.

(7) Lamboy, M. *Sedimentology* **1993**, *40*, 53.

(8) Simpson, D. R. *Am. Mineral.* **1964**, *49*, 363.

(9) Roy, D. M.; Linnehan, S. K. *Nature* **1974**, *247*, 220.

(10) Roy, D. M. U.S. Patent 3,929,971, 1975.

(11) White, E.; Shors, E. C. *Dent. Clin. North Am.* **1986**, *30*, 49.

(12) Ohgushi, H.; Okumura, M.; Yoshikawa, T.; Inoue, K.; Senpuku, N.; Tamai, S.; Shors, E. C. *J. Biomed. Mater. Res.* **1992**, *26*, 885.

(13) White, E. W. U.S. Patent 4,861,733, 1989.

(14) Eysel, W.; Roy, D. M. *Z. Kristal.* **1975**, *141*, 11.

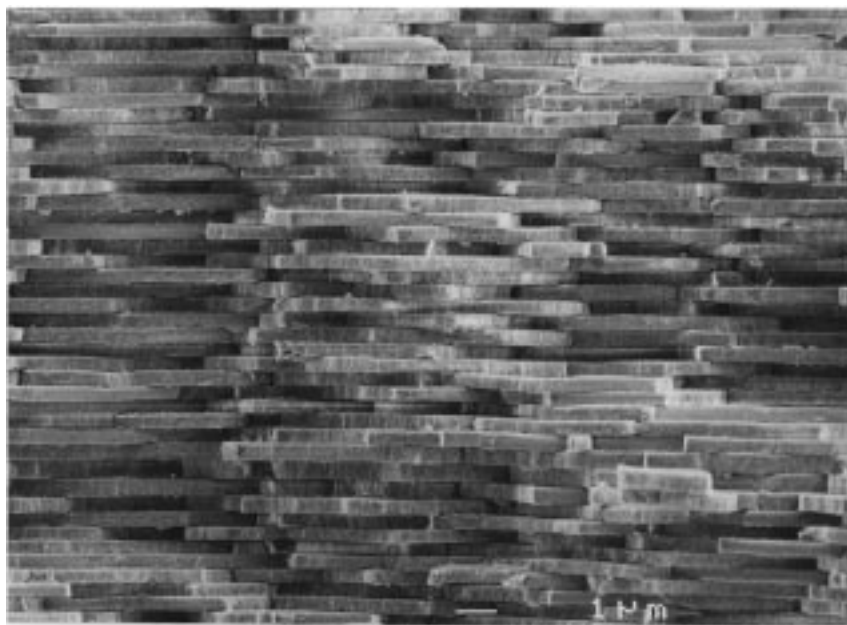


Figure 1. SEM image of a cross section of native gastropod (red abalone) nacre.

the original aragonite and the HA product are well-aligned.¹⁴

Nacre is the inner pearly layer of most mollusc shells. Nacre was converted to HA because it has properties common to both coral skeleton and geological aragonite yet has a nanoscale-ordered, brick-wall-like ultrastructure. This structure comprises *ab*-face single-crystal tablets of aragonite in composite with 1–5 wt % organic matter¹⁵ with a resulting fracture toughness $\sim 3 \times 10^3$ times greater than that of pure aragonite.^{16,17} In gastropod (red abalone) nacre, the aragonite tablets are 400 nm thick, 5–10 μm wide, and packed in flat sheets parallel to the shell surface and interlocking *c*-axis stacks normal to the shell surface (Figure 1).^{18–20} The nacre grows in cone-shaped stacks of tablets^{20,21} interspaced with thin (10–50 nm),²² fenestrated (97 pores/ μm^2),^{23,24} horizontally continuous organic sheets,^{21,24} collectively termed the *organic matrix*, which have both soluble and insoluble components.^{15,25–28} In mature

nacre, each tablet is encapsulated with an organic matrix^{21,24,29} and contains occluded within it a polyanionic protein.²⁷

This paper is the first report of the conversion of CaCO_3 in nacre to another inorganic within its ordered, interpenetrating organic matrix. In nature, minerals that undergo alteration within organic frameworks include HA in bone,^{30,31} iron oxides in the teeth of certain molluscs,³² and amorphous silica in plants and algae.²⁵ Conversion of nacre to HA may relate to inorganic conversions in other biominerals and reveal the effect of an interpenetrating organic matrix on inorganic reactions.

Finally, HA-converted nacre may have biomedically useful properties. Flat, *ab*-face pieces of both nacre³³ and HA³⁴ induce bone formation by osteoblasts in vitro; bivalve nacre can be fashioned into a strong, long-lasting dental root prosthesis.³⁵ Therefore, a material with the nacre ultrastructure and HA composition may be useful for either in vivo or in vitro bone growth studies.

Experimental Procedure

Sample Preparation. CaCO_3 samples converted to hydroxyapatite (HA) include gastropod (red abalone) nacre and prismatic calcite (*Haliotis rufescens*; marine gastropod mollusc, central California),¹⁸ coral skeleton (*Porites compressa*; scleractinian coral, Hawaii), bivalve nacre and prismatic calcite (*Atrina serrata*; Florida), nacre of another bivalve to confirm bivalve results (*Atrina* sp.; Baja, Mexico, data not presented in paper), cephalopod nacre (*Nautilus pompilius*), crabshell

(15) Weiner, S. *CRC Crit. Rev. Biochem.* **1986**, *20*, 365.

(16) Currey, J. D. *Proc. R. Soc. London, B* **1977**, *196*, 443.

(17) Jackson, A. P.; Vincent, J. F. V. *J. Mater. Sci.* **1990**, *25*, 3173.

(18) Zaremba, C. M.; Belcher, A. M.; Fritz, M.; Li, Y.; Mann, S.; Hansma, P. K.; Morse, D. E.; Speck, J. S.; Stucky, G. D. *Chem. Mater.* **1996**, *8*, 679.

(19) Manne, S.; Zaremba, C. M.; Giles, R.; Huggins, L.; Walters, D. A.; Belcher, A.; Morse, D. E.; Stucky, G. D.; Didymus, J. M.; Mann, S.; Hansma, P. K. *Proc. R. Soc. London, B* **1994**, *256*, 17.

(20) Wise, S. W. *Ecol. Geol. Helv.* **1970**, *63*, 775.

(21) Nakahara, H.; Bevelander, G.; Kakei, M. *Venus* **1982**, *41* (1), 33.

(22) Sarikaya, M.; Aksay, I. A. In *Results and Problems in Cell Differentiation*; Case, S. T., Ed.; Springer-Verlag: Berlin, 1992; Vol. 19, p 1.

(23) Schäffer, T. E.; Ionescu-Zanetti, C.; Proksch, R.; Fritz, M.; Walters, D. A.; Almqvist, N.; Zaremba, C. M.; Belcher, A. M.; Smith, B. L.; Stucky, G. D.; Morse, D. E.; Hansma, P. K. *Chem. Mater.* **1997**, *9*, 1731.

(24) Nakahara, H. In *Mechanisms and Phylogeny of Mineralization in Biological Systems*; Suga, S.; Nakahara, H.; Kaigi, N. G., Eds.; Springer-Verlag: Tokyo, 1991; p 343.

(25) Mann, S. *Nature* **1988**, *332*, 119.

(26) Cariolou, M. A.; Morse, D. E. *J. Comput. Physiol. B* **1988**, *157*, 717.

(27) Belcher, A. M.; Wu, X. H.; Christensen, R. J.; Hansma, P. K.; Stucky, G. D.; Morse, D. E. *Nature* **1996**, *381*, 56.

(28) Shen, X.; Belcher, A. M.; Hansma, P. K.; Stucky, G. D.; Morse, D. E. *J. Biol. Chem.* **1997**, *272*, 32472.

(29) Nakahara, H. *Venus* **1979**, *38*, 205.

(30) Glimcher, M. J. *Philos. Trans. R. Soc. London, B* **1984**, *304*, 479.

(31) Williams, R. J. P. *Philos. Trans. R. Soc. London, B* **1984**, *304*, 411.

(32) Mann S. In *Origin, Evolution, and Modern Aspects of Biomineralization in Plants and Animals*; Crick, R. E., Ed.; Plenum: New York, 1991; p 273.

(33) Lopez, E.; Vidal, B.; Berland, S.; Camprasse, S.; Camprasse, G.; Silve, C. *Tissue Cell* **1992**, *24* (5), 667.

(34) Sautier, J.-M.; Nefussi, J.-R.; Forest, N. *Cells Mater.* **1991**, *1* (3), 209.

(35) Camprasse, S.; Camprasse, G.; Pouzol, M.; Lopez, E. *Clin. Mater.* **1990**, *5*, 235.

Table 1. Experimental Parameters for Aragonite-HA Conversion

heating system	reaction vessel	aragonite mass, g	(NH ₄) ₂ HPO ₄		temp, °C	pressure	time
			solid, g	satd soln, g			
LECO/TEM-PRES HR-1B	sealed gold tube, 2 mL (6.3 mm diameter, 3 in. long)	0.13	0.32	0.79	215–260	0.8–2.1 kbar	6 h to 3.5 days
oven	bomb reactor, acid digestion (Parr, 23 mL) or custom-built (45 mL)	0.05–0.3	5.0	19.0	140–215	4–21 bar ^a	13 h to 4 weeks
oven	PTFE bottle, 60 mL	0.3	5.0	19.0	100	1 bar ^a	3 weeks to 6 mo
oven ^b	PTFE bottle, 60 mL	1	1.5	4.0	100	1 bar ^a	2 weeks

^a Vapor pressures for pure water at these temperatures; actual pressures are lower because highly saturated solutions were used.

^b Powder reagents were used in these experiments; whole bimineral pieces were used for all others. PTFE: polytetrafluoroethylene.

(California), spiny lobster shell (*Panulirus interruptus*; California), chicken eggshell, and geological aragonite.

Gastropod (red abalone) nacre, from shells of recently deceased animals (<1 year), was cleaved parallel to the shell surface with a heavy hammer. Flat pieces 0.3–0.6 mm thick, 1–4 mm wide, and 6–10 mg each were selected that lacked non-nacre heterolayers.¹⁸ Excluding coral skeleton, other CaCO₃ biominerals were prepared in the same manner. Freshly harvested coral skeleton was stored for up to 9 months in 75 vol % ethanol. After air-drying, the outer polyp-containing green layer was removed with a scalpel. The remaining white skeleton was broken with a hammer and 2–4-mm pieces, 5–10 mg each, were selected. A single crystal of geological aragonite 26 mm in diameter (*ab*-face) was cut with a low-speed saw (Buehler Isomet) into *ab*-face slices 0.6 mm thick, then cleaved in 1–4-mm-wide pieces with a razor blade.

Bleach-dispersed nacre tablets were prepared by ultrasonication of 1–15-mm-wide pieces of gastropod (red abalone) nacre devoid of non-nacre heterolayers¹⁸ in purified grade 4–6% sodium hypochlorite (bleach) for 2–3 days in 60 mL poly(tetrafluoroethylene) (PTFE) bottles with daily replacement of bleach followed by thorough rinsing in deionized water, filtration, and air-drying.

In Table 1, experimental parameters as a function of heating system are listed. Reaction products were rinsed thoroughly with deionized water and methanol and then air-dried.

X-ray Diffraction. The exterior surface of HA-converted nacre pieces was assessed for preferred orientation by one-dimensional (1-D) X-ray diffraction (XRD, Scintag PAD X) with Cu K α radiation at 45 kV, 40 mA in Θ – Θ geometry. 0.2°/min scans of 3–60° 2θ were collected from flat samples. The bulk of HA-converted biominerals was assessed for preferred orientation by two-dimensional (2-D) XRD (Siemens SMART with CCD area detector) with Mo K α radiation at 45 kV, 30 mA with a beam diameter of 0.5 mm. Exposures of 5–10 min were made on stationary samples 4.9 cm in front of the detector.

Integrations of the 2-D patterns were performed with GADDS software (3.2) for the Siemens HI–STAR detector system. Integrations were performed on only the (002) reflection of HA because it is intense and separate from other peaks. Integrations were fitted to Gaussian distributions (Jandel Scientific Peakfit) to measure preferred orientation.

To assess phase purity and crystal structure properties, 1-D XRD was conducted with samples ground to a powder with Si standard for lattice indexing. For conversion completion, patterns were collected from 25.6° to 27.6° 2θ at 0.1°/min. This region contains the (002) peak of HA and the strongest [(111)] and third strongest [(021)] peaks of aragonite; a minimum of 2–3% aragonite in HA can be detected. For converted gastropod nacre, reaction completion was further confirmed in 2-D XRD patterns by the absence of (111) aragonite reflections (prominent for native nacre) and in Fourier transform infrared (FTIR) spectra (described below) by the absence of the ν_4 mode of CaCO₃ at 720 cm⁻¹ (Figure 10).³⁶

To assess the possibility of topotactic transformation to HA in gastropod nacre, the crystal structure of aragonite was

modeled with Insight II (3.0) Solids Builder (6.0) and a lattice search program.³⁷ Pseudo-hexagonal unit cells of aragonite with *ab*-planes parallel to the orthorhombic *c*-axis of aragonite were found and compared with the hexagonal lattice of HA.¹⁴

Scanning Electron Microscopy (SEM). SEM was conducted with a cold cathode field-emission source (JEOL JSM-6300F) on samples either uncoated or sputter-coated with 200 Å Au/Pd. Images of cross-section fractures were prepared as follows. Tough or thick native shell phases (Figures 1 and 7g) were fractured by striking the plane of the shell surface with a heavy hammer. Weak or thin native shell phases (Figure 7a,c,e) and all HA-converted biominerals were fractured by breaking the samples in two pieces between two wide-tipped tweezers. Fractured samples were affixed to the walls of specimen mounts with their fracture surfaces facing up.

Other Techniques. Thermal gravimetric analysis (TGA) and differential thermal analysis (DTA) were conducted simultaneously in air or oxygen with 50–100 mg samples ground to 115 mesh (Netzsch STA-409, DTA referenced to calcined Al₂O₃, heating rate 10°/min). For reproducibility, three different samples were dried overnight in a vacuum oven at 80 °C and replicate TGA were conducted on a different system (Mettler TA 3000). FTIR spectroscopy (Mattson Instruments Galaxy system) was conducted with 0.3-mm-thick pieces of HA-converted nacre and coral skeleton ground and pressed in KBr disks (0.9 mg of sample/200 mg of KBr) at 1.2–1.3 kbar pressure for 15 min. Vickers microhardness testing of HA-converted nacre was conducted with flat samples glued to glass slides using a Tukon microhardness tester (Page-Wilson) with 200 g loads.

Results

Bulk Kinetics. All products have the hydroxyapatite (HA) crystal structure with no other phases of calcium phosphate. Although it was expected that the organic matrix of biominerals might facilitate conversion to HA at organic-preserving temperatures (<150 °C), at the lowest temperature of 100 °C neither gastropod nacre nor coral skeleton pieces convert to HA. Instead, at 100 °C HA particles of irregular shape 100–800 nm wide are released from the starting material increasingly with time. At >140 °C, although a portion of the sample (~11 wt %) is released as loose HA powder, sample form is largely retained; for gastropod nacre this reaction requires 1 month at 140 °C (Figure 2). Yet it is surprising that HA-converted gastropod nacre retains its form at all; both bivalve and cephalopod nacre are destroyed to HA powder by this reaction at any temperature. Therefore, unless otherwise specified, HA-converted nacre refers only to gastropod nacre.

Temperature, time, and volume of reaction solution affect the conversion rate more than pressure. For example, because the solution volume/sample ratio is

(36) LeGeros, R. Z.; LeGeros, J. P.; Trautz, O. R.; Klein, E. *Dev. Appl. Spectrosc.* **1970**, *78*, 3.

(37) Program written and executed by Clayton Otey as a UCSB RISE summer intern, now at the California Institute of Technology.

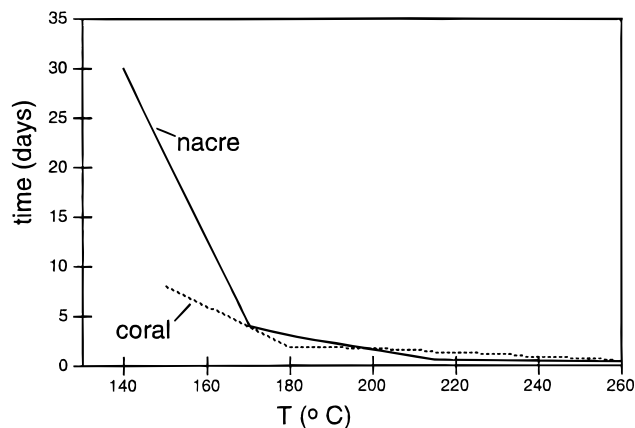


Figure 2. Plot of time versus temperature for equal-mass samples of gastropod nacre and coral skeleton to convert to HA. Significant divergence in rate occurs only at $<170^{\circ}\text{C}$.

higher in bomb reactors than in gold tubes (Table 1), in the former at 215°C (21 bar) nacre is completely converted in 13 h, but in the latter at 215°C (1 kbar) nacre is largely unreacted in 13 h, despite the significantly higher pressure. In gold tubes at the higher temperature of 260°C , however, full conversion requires only 6–8 h, despite the low solution volume/sample ratio. Because these results show that temperature and time most critically affect reaction rate, in Figure 2 samples are plotted with these parameters only.

At 260°C , 1 kbar, gastropod nacre converts to HA 28 times more rapidly than geological aragonite of identical size,¹⁴ despite being only 7.2% less dense. This may occur because nacre has a high internal surface area which is accessible through its interconnecting organic matrix. Although gastropod nacre is $\sim 31\%$ more dense than coral skeleton, at $>170^{\circ}\text{C}$ they convert to HA with similar rates (Figure 2). At $<170^{\circ}\text{C}$, however, coral skeleton converts to HA more quickly; at 150°C , its conversion rate is three times faster than that of nacre (Figure 2). This shows that at lower temperatures the surface area of nacre is less accessible than that of the more porous coral skeleton.

Crystallographic Orientation. On the exterior surface of HA-converted nacre, 1-D XRD reveals completely random orientation (data not shown). However, through the bulk of HA-converted nacre, 2-D XRD reveals substantial preferred orientation (Figures 3a and 4a). 2-D XRD patterns were interpreted as follows. The scattering angle with respect to the primary beam is 2θ ; its direction (shown in Figure 3a) is radial from the beam center. Integration of 2θ over pie-slice-shaped regions gives conventional powder patterns of intensity versus degrees 2θ (Figure 3).

χ is the circular direction around a diffraction ring. A 360° integration of the (002) ring of HA is plotted as intensity versus degrees χ in Figure 4. The full width at half-maximum (fwhm) of peaks in this plot gives a measure of preferred orientation (Table 2). The percentage of crystallites in a particular orientation (Table 2) is calculated by subtracting the intensity in 2θ of the randomly oriented HA background from that of the oriented HA and integrating over the peak in χ .

In native nacre, the aragonite c -axis is perpendicular to the plane of the shell surface with high c -axis

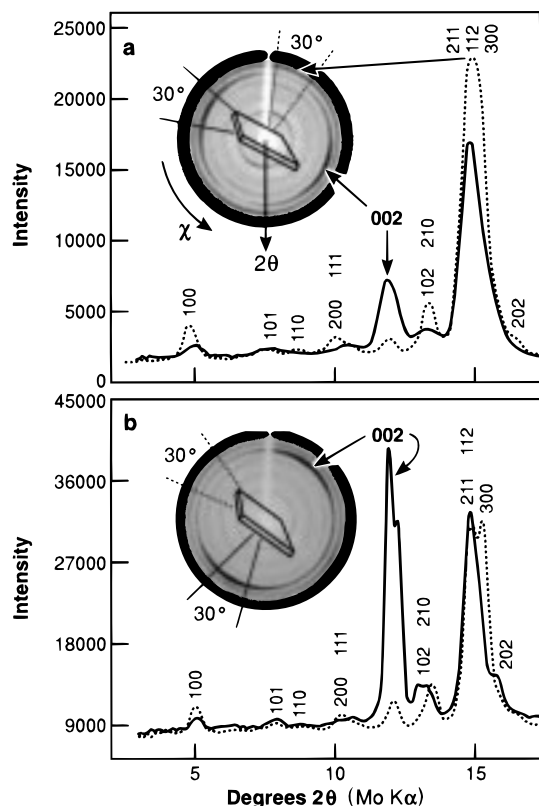


Figure 3. 2-D XRD patterns and integration plots over 30° regions in χ (indicated) plotted as intensity versus degrees 2θ for (a) HA-converted nacre (140°C , 4 bar, 1 mo) and (b) HA-converted ab -face geological aragonite (260°C , 0.8 kbar, 24 h). Indexed Bragg reflections are shown. Plate-shaped samples were oriented in edge-view geometry with the plane of the sample $\sim 45^{\circ}$ from vertical, as shown. Preferred orientation is most evident in the (002) reflection (indicated), with solid and dashed lines corresponding to the most and least oriented regions of the (002) reflection, respectively.

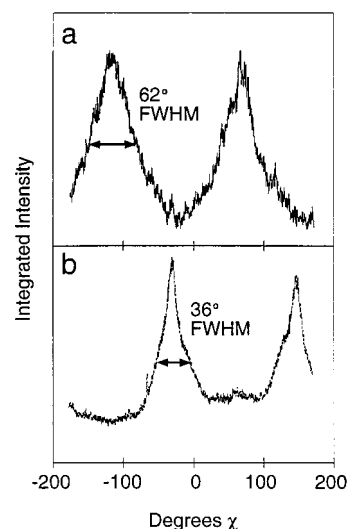


Figure 4. 360° integrations in χ of the (002) reflection in Figure 3a,b plotted as integrated intensity versus degrees χ . The integrations proceed counterclockwise from the vertical beam stops in Figure 3 and contain approximately Gaussian peaks that comprise 72% of the crystallites (a) and 66% (b).

alignment.^{19,38} Accordingly, in 2-D XRD patterns of

(38) Sarikaya, M.; Gunnison, K. E.; Yasrebi, M.; Aksay, I. A. *Mater. Res. Soc. Symp. Proc.* **1990**, *174*, 109.

Table 2. Orientation Data from Gaussian Distributions of the (002) Peak of HA^a

sample	% perpendicular \pm 5%	% parallel \pm 5%	% random \pm 5%	fwhm \pm 2°	
				perpendicular	parallel
Gastropod Nacre					
140 °C, 3 weeks (a)	32	0	68	48	NA
140 °C, 4 weeks (b)	52	0	48	55	NA
220 °C, 13 h (c)	50	0	50	58	NA
260 °C, 6–12 h (d)	33	16	55	39	23
260 °C, 2–3.5 days (b)	52	4	44	27	25
Other CaCO ₃					
geological aragonite (c), 260 °C, 24 h	0	66	34	NA	36
gastropod prismatic calcite (c)	0	44	56	NA	125
lobster shell (c)	0	25	76	NA	112
eggshell (a)	0	23	77	NA	56
coral skeleton, 260 °C, 6 h (c)	0	0	100	NA	NA

^a Average of (a) two, (b) five, (c) one, and (d) eight samples. NA: not applicable. Where no conversion conditions are given, samples were prepared at 200–210 °C for 1–2 days.

native nacre (not shown), the aragonite (002) reflection is perpendicular to the plane of the sample with a narrow fwhm of 9.2° χ . No randomly oriented aragonite is detected.

After conversion, however, the (002) ring of HA contains either one or two different preferred orientations. In the *parallel* orientation, the *c*-axis of HA is parallel to the *c*-axis of the original aragonite and the (002) reflection is strong perpendicular to the plane of the sample (Figure 3b). In the *perpendicular* orientation, the *c*-axis of HA is perpendicular to the *c*-axis of the original aragonite and the (002) reflection is strong in the plane of the sample (Figure 3a).

Expression of these orientations is dependent on reaction temperature and time. At the lowest temperature of 140 °C, only the perpendicular orientation is observed (Figure 3a) with a broad fwhm of 55° χ (Figure 4a, Table 2). At the highest temperature of 260 °C, the perpendicular and parallel orientations coexist, with the perpendicular orientation increasing approximately linearly with time. For example, in 6–12 h, more than twice as much HA is perpendicular (33%) than parallel (16%); in 2–3.5 days, 52% is perpendicular and only 4% is parallel (Table 2). This suggests that with time, parallel-oriented HA dissolves and recrystallizes with perpendicular orientation.

In addition, with temperature and time, the alignment of perpendicular-oriented HA increases (Table 2). In 6–12 h at 260 °C, the perpendicular (002) peak has a fwhm of 39° χ . In 2–3.5 days, this peak is 31% narrower at 27° χ . The alignment at 260 °C increases linearly from 6 h to 2 days and then changes negligibly from 2 to 3.5 days (data not shown).

In contrast, the alignment of parallel-oriented HA changes negligibly with time. Instead, with time its yield diminishes to zero (Table 2).

Ultrasonication in bleach of HA-converted nacre yields irregular crystallites 150–350 nm wide. These are the smallest components of HA-converted nacre which, in aggregate, comprise the converted tablets shown in Figures 5 and 6. To characterize their crystallographic orientation, the crystallites were ex-

amined by electron diffraction.³⁹ Because prior to bleach treatment the intact sample analyzed contained 59% perpendicular-oriented crystallites, it was expected that a majority of the bleach-dispersed crystallites would be elongated along the *c*-axis (HA growth direction)^{40,41} and thus might include the *c*-axis in their reciprocal lattices. However, results were inconclusive because the crystallites analyzed could be indexed to several different zone axes, none of which included the *c*-axis.

Morphology. In native gastropod nacre, cross-section fractures traverse the organic matrix between stacks of tablets (Figure 1).^{42–44} In HA-converted nacre, although the organic phase is largely degraded by conversion conditions (Table 3), cross-section fractures follow the same path between stacks of tablets, and both tablet and stacks-of-tablets morphologies are preserved (Figure 5). Even the interdigitation of tablets is intact (Figures 5c–f). In cross-section fractures, these preserved features are more evident in the core of the sample than at the edges, where there is less regular structure (not shown). Indeed, SEM images of the exterior surface reveal irregular nanocrystallites with no aggregate features.

SEM data suggest that the extratable organic matrix is degraded before the tablets are converted. Cross-section fractures reveal that the hydrothermal solution may travel between stacks of tablets in 0.9–1.5- μ m-wide channels up to 54 μ m long that trace the edges of the interdigitating tablets (Figure 5b). Indeed, the interdigitation of tablets, which in native nacre creates tablet-edge overlaps 0.4–2.0 μ m wide, may bind the converted nacre together despite degradation of the organic phase. The product is therefore robust; ultrasonication in bleach for at least 8 h is required to disperse the material into its component nanocrystallites.

(39) HA-converted nacre (260 °C, 3.5 days) was placed in a 1.5 mL microcentrifuge tube filled with bleach, subjected to 8 h of ultrasonication, rinsed thoroughly in 10 000 molecular weight cutoff dialysis tubing, filtered, suspended in ethanol, deposited on a Cu grid, and examined with a JEOL 2000 fx electron microscope. An attempt was made to index the electron diffraction patterns with IdealMicroscope (1.2, EMLabs).

(40) Roy, D. M. *Mater. Res. Bull.* **1971**, *6*, 1337.

(41) Eysel, W.; Roy, D. M. *J. Cryst. Growth* **1973**, *20*, 245.

(42) Gunnison, K. E.; Sarikaya, M.; Liu, J.; Aksay, I. A. *Mater. Res. Soc. Symp. Proc.* **1992**, *255*, 171.

(43) Sarikaya, M. *Microsc. Res. Technol.* **1994**, *27*, 360.

(44) Jackson, A. P.; Vincent, J. F. V. *J. Mater. Sci.* **1990**, *25*, 3173.

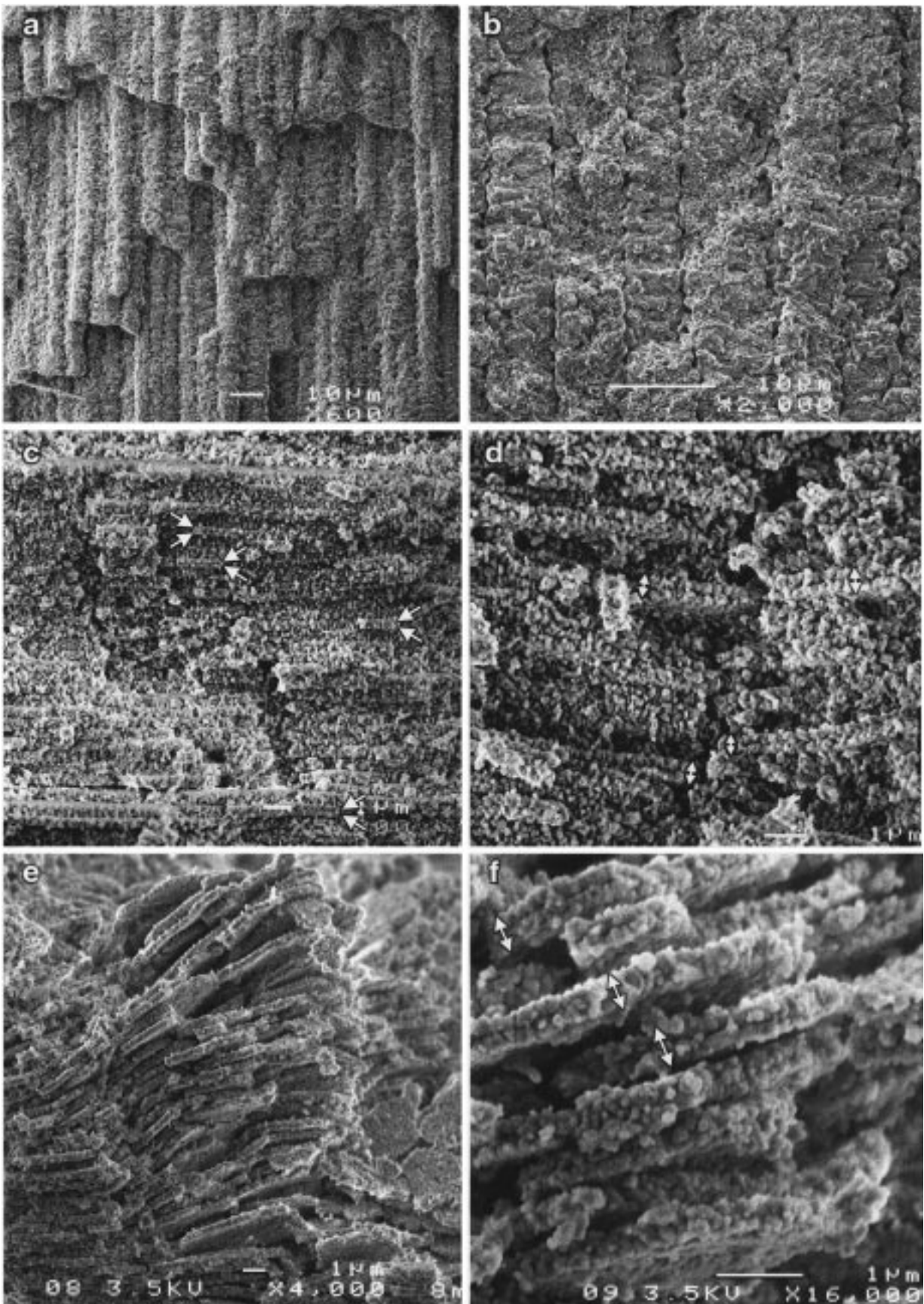


Figure 5. SEM images of cross-section fractures through the bulk of nacre pieces fully converted to HA at 260 °C, 1 kbar: (a–c) treated for 8 h, (d) for 12 h, and (e–f) for 3.5 days. Panels a and b show rigid stacks of tablets, panels c–f show that many tablets comprise bilayers of nanocrystallites with the most prominent indicated by arrows, and panel e shows that after prolonged reaction time, stacks are weakly bound yet tablets remain intact.

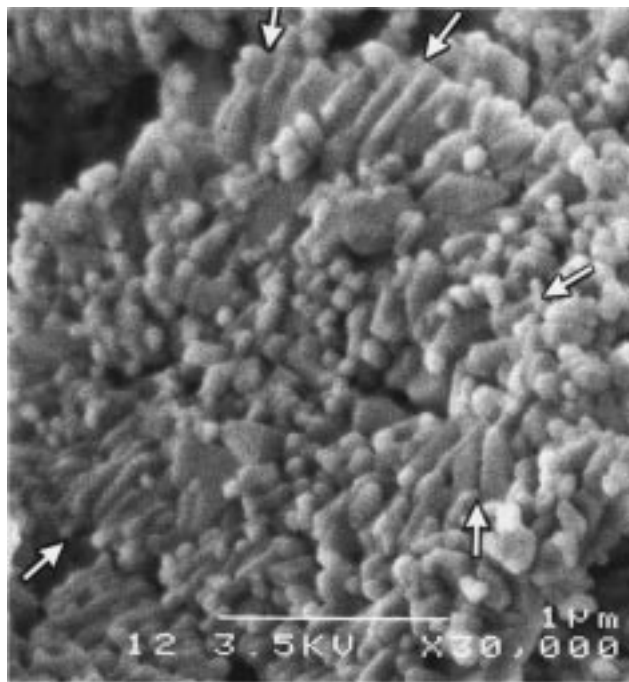


Figure 6. Plan-view tablet of HA-converted nacre, enlarged from the lower right of Figure 5e, where several tablets were dislodged during cross-section fracture. Arrows indicate directions of the long axes of approximately radially oriented crystallites.

HA-converted nacre has an off-white color and lack of iridescence consistent with enhanced light scattering by an aggregate of nanocrystallites, as opposed to the regularly ordered micron-scale crystals of native nacre. In addition, the lamellae (horizontal sheets) of HA-converted tablets are sometimes not straight, as in native nacre (Figure 1), but instead have undulating curvature, possibly induced by fracture (Figure 5e). In some fracture cross-sections, tablets have emerged from the ultrastructure and, surprisingly, are whole (Figures 5e and 6).

During HA conversion, tablets are transformed from 400-nm-thick single crystals of aragonite (Figure 1) to, in many cases, 300–600-nm-thick bilayers of HA crystallites 30–800 nm wide (Figures 5c–f). These are most readily observed at 260 °C. In plan views of converted tablets, elongated crystallites are observed with their long axes oriented approximately radially about the tablet center (Figure 6). Because the *c*-axis is the customary growth axis of HA,^{40,41} these crystallites may have grown from the tablet periphery inward.

With reaction time, the crystallites lengthen. For example, in 8 h at 260 °C, the crystallites in a tablet are 200–800 nm long (not shown); in 3.5 days at 260 °C, they are 450–800 nm long (Figure 6).

Geological Aragonite and Other CaCO₃ Biominerals. It was previously reported that *ab*-face slices of geological aragonite convert to HA (260 °C, 1–3 weeks) with almost complete preservation of both sample form and crystallographic orientation, although the product is polycrystalline.¹⁴ In our studies, however, in an *ab*-face slice of geological aragonite, ~20% converted to HA (260 °C, 24 h), only 66% of the HA had the “preserved” parallel orientation and 34% had random orientation (Table 2). The morphology comprised wavy, elongated rods 0.1–0.3 μm wide and up to 0.8 μm

long (not shown). These results suggest that for HA conversion, high preferred orientation is a result of prolonged dissolution–recrystallization.

In native coral skeleton, 80–200-μm-wide walls enclose 0.1–0.2-mm-wide channels (not shown). SEM reveals that the walls comprise 0.25–0.5-μm-wide elongated crystallites with typical aragonite morphology. After conversion to HA (140–260 °C), the wall dimensions are unchanged.⁹ Within the walls, however, the crystallites have hexagonal-plate morphologies from 50 nm to 0.8 μm wide (not shown). Both the hexagonal shape and the monodispersity of the crystallites increase with temperature. However, no detectable change in preferred orientation accompanies conversion; both native and HA-converted coral skeleton are randomly oriented.

Surprisingly, perpendicular-oriented HA was found only in converted gastropod nacre. Although gastropod prismatic calcite, lobster shell, and eggshell convert completely to HA at the same reaction temperature and time (210 °C, 24 h) as gastropod nacre and also retain their sample form, these converted biominerals contain only parallel-oriented HA, i.e. with its *c*-axis parallel to the *c*-axis of the original CaCO₃ and perpendicular to the plane of the shell surface (Table 2). Moreover, in these converted biominerals, the average quantity and preferred alignment of parallel-oriented HA is approximately one-half and one-fourth those of parallel-oriented HA in gastropod nacre converted under identical conditions, respectively (data not shown).

In addition, these biominerals lose their ultrastructure during HA conversion. In eggshell, 80–100-μm-diameter calcite prisms (Figure 7e) convert to HA with a gridwork of variously oriented 0.2–3.2-μm-diameter rods (Figure 7f). Gastropod prismatic calcite (*Haliotis rufescens*) converts from calcite prisms 100–200 μm in diameter (Figure 7g)^{18,45} to a densely packed aggregate of 0.5–6-μm-wide fibers (Figure 7h). This product has 48% greater orientation than converted eggshell (Table 2), perhaps due to the original arrangement of organic, which in native gastropod prismatic calcite is unevenly distributed so that no distinct prism boundaries are apparent (Figure 7g).⁴⁵ Ultrasonication of this native material with bleach fails to release single prisms but instead releases isotropic granules 3.5 μm in diameter (not shown). This suggests that organic sheets subdivide the prisms⁴⁵ and, during conversion to HA, may strategically direct the hydrothermal solution through the ultrastructure.

In another surprising comparison, bivalve nacre (*Atrina serrata*) disintegrates to a loose powder of rods during HA conversion, regardless of temperature (180–250 °C tested) and time (occurs in as little as 4 h at 250 °C). The rods are 70–430 nm wide and 0.38–1.4 μm long (Figure 7b). Bivalve prismatic calcite also disintegrates during conversion, although it forms long fibers with a much higher aspect ratio (50–900 nm wide, 0.4–10.4 μm long) that, when filtered, overlap to create a weakly bound fibrous sheet (Figure 7d). *Nautilus* nacre and crabshell also disintegrate to powder during HA

(45) Mutvei, H. In *Origin, Evolution, and Modern Aspects of Biomineralization in Plants and Animals*; Crick, R. E., Ed.; Plenum: New York, 1991; p 137.

Table 3. Thermal Gravimetric Data for Native and HA-Converted Biominerals^a

sample	total organic		organic 1		organic 2	
	wt %, ± 0.3	T _{loss} , °C, ± 5	wt %, ± 0.3	T _{loss} , °C	wt %, ± 0.3	T _{loss} , °C
Native Biominerals						
gastropod nacre (a)	3.8	150–440	3.3	150–380	0.5	380–440
bleach-dispersed nacre tablets (b) (gastropod)	0.41	180–425	0.15	150–300	0.3	300–415
bivalve nacre (c)	3.4	150–425	2.6	150–330	0.8	330–425
coral skeleton (d)	2.4	150–440	1.0	150–290	1.3	290–440
gastropod prismatic calcite (c)	4.5	145–480	NA	NA	NA	NA
HA-Converted Biominerals						
coral skeleton 150 °C, 13 days (c)	0.76	140–475	0.36	140–320	0.4	320–475
gastropod nacre 140 °C, 1 mo (c)	0.27	275–475	NA	NA	NA	NA
gastropod nacre 180 °C, 2 days (c)	0.80	200–470	NA	NA	NA	NA
gastropod nacre 180 °C, 5 days (c)	0.53	240–510	NA	NA	NA	NA
gastropod nacre 180 °C, 6 days (c)	0.38	250–480	NA	NA	NA	NA

^a Average of (a) three, (b) six, (c) one, and (d) four samples. NA: not applicable.

conversion, resulting in equant particles 130–800 nm and 30–350 nm wide, respectively (not shown).

Thermal Properties of Native Biominerals. Thermal analyses were used to quantify organic content. TGA/DTA plots of native gastropod nacre and coral skeleton contain three regions of weight loss: (i) the endothermic loss of physically adsorbed water at 40–150 °C, (ii) the exothermic loss of organics at 150–440 °C, and (iii) the endothermic loss of CO₂ at 620–840 °C (Figure 8, Table 3).

Gastropod nacre and coral skeleton contain an average of 3.8 and 2.4 wt % organic, respectively. In the nacre, the organic lowers its density to 2.7180(8) g/cm³.⁴⁶ This value is 7.2% lower than that of pure aragonite [2.930(4) g/cm³],⁴⁷ a difference which is on the order of the organic content of 3.8% (Table 3).

In both gastropod nacre and coral skeleton, the organic is released in two separate weight losses, *organic 1* and *organic 2*, which have different rates of weight loss and separate exothermic peaks in the DTA plot (Figure 8). In nacre, *organic 1* comprises 87% of the total organic and is released at a faster rate and over a greater temperature range than *organic 2*. In coral skeleton, organics 1 and 2 are more nearly equal at 42 and 54% of the total organic, respectively, and are released over equivalent temperature ranges of 145°.

The thermal data show that in gastropod nacre, *organic 1* is extracrystalline organic matrix and *organic 2* is a water-soluble, polyanionic protein that is occluded within the tablets during their formation.²⁷ Thermal plots of bleach-dispersed nacre tablets, with virtually all extracrystalline organic removed,⁴⁸ are dominated by a single exothermic loss of 0.3 wt % at 300–415 °C (Table 3). This loss is roughly equivalent in both quantity and temperature range to *organic 2* in native nacre, although it occupies a broader temperature range and commences at an earlier temperature, possibly because *organic 1* has been removed.

Gastropod nacre contains only 13% more organic than bivalve nacre (Table 3). In both, the organics exhibit two-part weight losses at roughly equivalent tempera-

tures and rates. The main difference is that in bivalve nacre, *organic 2* comprises 24% of the total organic (compared to 13% in gastropod nacre) and commences its weight loss at a 50° lower temperature. This may contribute to differences in the stability of these naces to HA conversion.

In contrast, in gastropod prismatic calcite the organic evolves in one rather than two steps (Table 3). This suggests that in this biomineral the extra- and intracrystalline organics are not physically separated enough to result in separate weight losses.

Thermal Properties of HA-Converted Biominerals. Thermal plots of HA-converted nacre and coral skeleton contain three regions of weight loss: (i) water at 40–180 °C, (ii) *organic 1* at 240–490 °C, and (iii) an endothermic loss of CO₂ and H₂O from the crystal structure of HA at 630–1200+ °C (Table 3).

Converted nacre contains 79–93% less organic than native nacre, depending on temperature and time. This residual organic exhibits a single-step weight loss that commences at a >50 °C higher temperature than the *organic 1* in native nacre (Table 3), which reflects that considerable thermal degradation has taken place.

It was expected that for conversions at low temperatures, the *organic 1* of nacre would be better preserved. However, the opposite is true: *organic 1* content decreases with lower temperature conversion because at low temperatures more time is required for complete conversion. This enables more thermal degradation to take place. Accordingly, the *organic 1* content of nacre converted at 180 °C decreases linearly with time from 2 to 6 days (Table 3). In addition, the initial temperature of *organic 1* weight loss increases with time, which indicates that the *organic 1* is increasingly degraded with time (Table 3).

Mechanical Properties. Although previous studies showed that HA-converted coral skeleton is harder than native coral skeleton,⁹ HA-converted nacre is approximately half as hard as native nacre, with hardness increasing linearly with temperature, as shown in Figure 9. In addition, the consistency in hardness values for samples from the same batch is more regular with temperature. Because HA has a Moh's hardness that is 50 times greater than aragonite, the decrease in hardness that accompanies HA conversion may be unrelated to the change in mineral phase and instead may relate to the smaller size of crystallites in the product and/or destruction of the binding *organic 1* phase.

(46) Density measurement was made on a Micromeritics AccuPyc 1330 system with nacre devoid of nonnacre heterolayers (see ref 18).

(47) Lide, D. R., Ed. *CRC Handbook of Chemistry and Physics*; CRC: Boca Raton, Florida, 1990; p 4-169.

(48) By SEM, bleach-dispersed native nacre contains either single tablets with the pretreatment dimensions or 0.2–2.2- μ m subtablet particles, depending on the extent of bleach treatment. However, no significant difference in *organic 1* quantity is observed after treatments of varying duration.

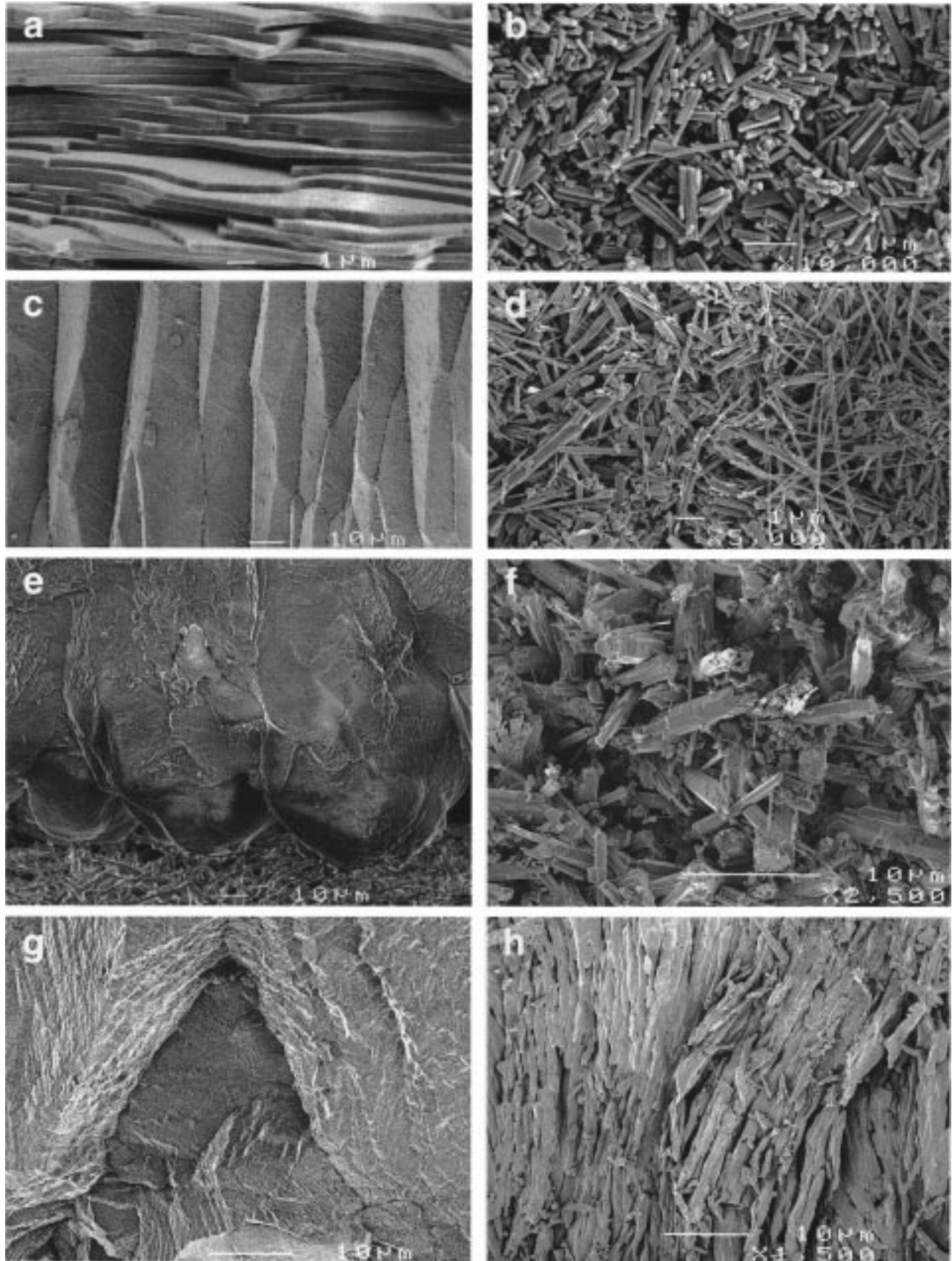


Figure 7. SEM images of native (left) and HA-converted (right) bivalve nacre (a, b), bivalve prismatic calcite (c, d), chicken eggshell (e, f), and gastropod prismatic calcite (g, h). None of the products retained the structure of the starting material. Panel b is a powder of rods, panel d a powder of needles, panel f a converted shell of rods, and panel h a converted shell of elongated fibers. In fracture cross sections (a, c, e-h), the plane of the shell surface is along the horizontal. Panels b and d comprise dispersed powder compacted in a filter cake.

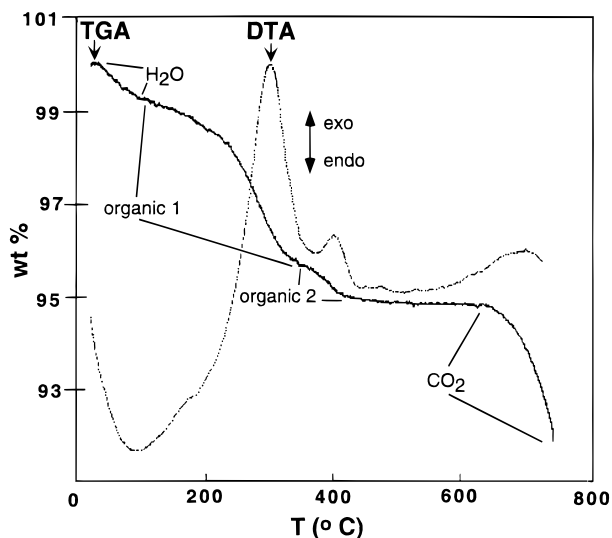


Figure 8. Thermogravimetric analysis (TGA) and differential thermal analysis (DTA) of native nacre in oxygen. The two organic weight losses (organics 1 and 2) have separate exothermic peaks in the DTA. Adsorbed water is released at 30–150 °C, organic 1 at 150–350 °C, organic 2 at 350–445 °C, and CO₂ at >640 °C.

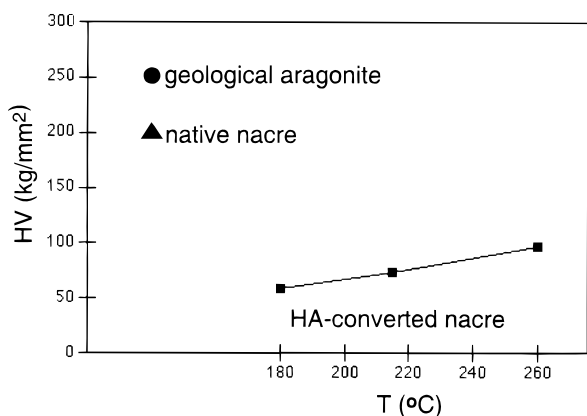


Figure 9. Hardness values (HV, Vickers) for *ab*-face geological aragonite and native nacre (not as a function of temperature) compared with HA-converted nacre (plotted vs temperature) prepared at 180–260 °C. Each value (± 5 kg/mm²) was obtained from 11–21 measurements collected from at least three samples.

Crystal Structure. HA-converted nacre and coral skeleton result in narrow XRD and FTIR peaks indicative of high crystal order/grain size. In the powder XRD patterns of both, the fwhm of the (002) peak decreases linearly with time at a particular temperature and also with temperature. For example, for nacre converted at 260 °C, the average fwhm decreases from 0.11° 2θ at 10 h to 0.09° 2θ at 50 h. This shows that crystal order/grain size increases with temperature and time.

HA converted from CaCO₃ and exposed to atmospheric CO₂ is expected to contain some CO₃²⁻ in its crystal lattice.^{4,36} In the FTIR spectra of nacre converted to HA at all temperatures, the ν_3 mode of CO₃²⁻ lies at 1460 and 1550 cm⁻¹ and the ν_2 mode lies at 880 cm⁻¹ (Figure 10). These values are suggestive of *type A/high temp* CO₃²⁻, located at OH⁻ sites in the HA lattice. For *type B/low temp* CO₃²⁻, located at PO₄³⁻ sites, these

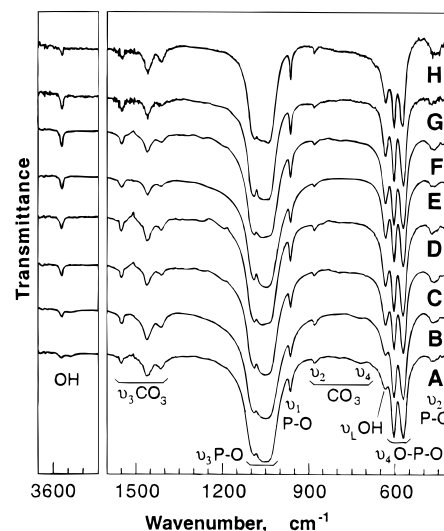


Figure 10. FTIR spectra of HA-converted nacre prepared at (a) 140 °C, 4 weeks, (b) 180 °C, 2 days, (c) 180 °C, 6 days, (d) 165 °C, 10 days, (e) 150 °C, 21 days, (f) 215 °C, 7 days, (g) 215 °C, 13 h, and (h) 260 °C, 3.5 days. Irregular trends with temperature and time arise from variations in sample size, shape, and location in the reaction vessel.

modes would instead lie at 1430, 1534, and 864 cm⁻¹.^{4,49}

The lattice constants of HA-converted nacre also are suggestive of *type A* CO₃²⁻. *Type A* CO₃²⁻ results in expansion of *a*; *type B* results in slight contraction of *a*.^{4,50} At 140 °C, *a* = 9.440(6) Å and at 260 °C, *a* = 9.433(5) Å (average values), both of which are expanded relative to pure HA (*a* = 9.417 Å).¹⁴ Compared to literature values of *a* for *type A* hydroxyapatite, these samples contain approximately 1.2 and 0.8% CO₃²⁻, respectively.³⁶ Moreover, *type A* CO₃²⁻ can be expelled by heating to 1000 °C.^{4,50,51} Accordingly, when HA-converted nacre is heated in air to 1300 °C, *a* decreases to 9.413(5) Å, which is nearly equivalent to that of pure HA (*a* = 9.417 Å). CO₃²⁻ is also expelled from HA-converted nacre with reaction time; at 140 °C, *a* contracts linearly from 9.453(5) Å in 10 days to 9.428(2) Å in 4 weeks.

FTIR spectra reveal that as CO₃²⁻ is expelled with time and temperature, OH⁻ content increases. In a series of differently treated samples, the least intense OH⁻ stretch at 3570 cm⁻¹ occurs at the lowest temperature of 140 °C (Figure 10A). From 2 to 6 days at 180 °C, both the OH⁻ libration at 630 cm⁻¹ and the OH⁻ stretch at 3570 cm⁻¹ increase in intensity (Figure 10A,B). In addition, with temperature and time the ν_1 phosphate band at 968 cm⁻¹ shifts to increasingly low frequency. This may be due to an increase in terminal P–O bonds adjacent to hydrogen-bonded P–O and thus supports increasing OH⁻ content with temperature and time.

Discussion

This paper demonstrates for the first time that the CaCO₃ of gastropod nacre can be converted hydrother-

(49) Roy, D. M.; Eysel, W.; Dinger, D. *Mater. Res. Bull.* **1974**, *9*, 35.

(50) Bonel, G.; Montel, G. *Compt. Rend.* **1964**, *258*, 923.

(51) Nadal, M.; Trombe, J. C.; Bonel, G.; Montel, G. *J. Schimi. Phys.* **1970**, *6*, 1161.

mally to HA not only with retention of sample form and internal ultrastructure but also with a unique new orientation that suggests the conversion occurs by dissolution–recrystallization, with increasing orientation with time. These results may be a consequence of the unique organization of the organic phase, which imparts a kinetic and orientational effect on the conversion. Although previous studies of the aragonite–HA conversion in geological aragonite supported a mechanism of solid-state topotaxy, they indicated that other processes could contribute.¹⁴ This was suggested because nonoriented slices of geological aragonite converted at a similar rate, but resulted in significantly more randomly oriented HA than *ab*-face slices.¹⁴

Our results show that gastropod nacre is unique among molluscan nacles in retaining its sample form during HA conversion. The two other types of molluscan nacre—bivalve and cephalopod—disintegrate to HA powder without converting through their bulk. This difference in behavior may stem from differences in the quantity of the organic, the composition and physical properties of the organic, and the structural arrangement of the organic through the composite material.

For example, in our experiments gastropod nacre contained 37% more organic matter than bivalve nacre. Of this organic material, 87% is located outside the tablets (organic 1, Table 3), where it encapsulates each tablet and connects it to the bulk; 13% of the organic is occluded within the tablets. In bivalve nacre, not only is there less total organic, but also only 76% is located outside the tablets (Table 3). Because HA-converted tablets resist intratable fracture and there are vertical channels where organic once resided (Figure 5), extratable organic may be degraded by the hydrothermal conditions before the tablets are converted. Therefore, the greater quantity of extratable organic in gastropod nacre may contribute to its stability.

The extratable organic in gastropod nacre may also be more heat-resistant. In thermal plots of gastropod nacre, this organic evolves until 380 °C; in bivalve nacre it evolves until only 330 °C (Table 3). Recent chemical analysis of Lustrin A, an insoluble extratable protein of red abalone nacre, suggests that it may have exceptional stability due to elastomeric linkages and extensive disulfide bonding of its high content of cysteine residues.²⁸

It has been suggested that the organic matrix of gastropod nacre has evolved to be tougher than that of bivalves and cephalopods because its brick-wall arrangement is more weakly designed.^{20,25} Although the latter forms of nacre resemble a true brick wall, with tablets centered largely on lateral boundaries between the tablets above and below, in gastropod nacre the tablets are stacked in vertical columns, with overlaps of only 0.4–2.0 μm between the 5–10- μm -wide tablets (Figure 1).

However, the columnar arrangement of tablets in gastropod nacre may be responsible for its unique stability to HA conversion. Figure 11 shows a schematic of vertical paths the reaction solution may take through cross sections of gastropod and bivalve nacre if one makes two assumptions: (i) the hydrothermal solution flows more readily through the organic matrix than the aragonite tablets, which are considerably more dense,

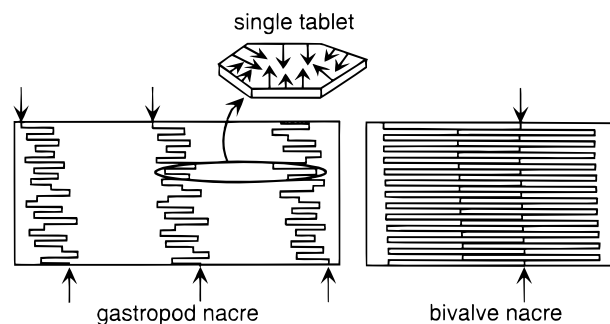


Figure 11. Schematic diagram of possible directions of reaction solution, shown by arrows, through cross sections of gastropod and bivalve nacre based on their organic matrix arrangement. Enlargement (above) shows radial directions of solution flow toward a single tablet in plan-view.

and (ii) the autogenous pressure directs the solution flow predominantly from the surface-normal direction, because the top and bottom sample surfaces have greater surface area than the sample edges.

In bivalve nacre, no direct vertical path through the material can be made; instead the solution travels between lamellae in the horizontal direction or around each tablet in the vertical direction (Figure 11), both of which can compromise the integrity of the material. As a result, converted tablets may be released into solution before the bulk is converted.

Instead, with gastropod nacre a zigzagging vertical path along the organic is available (Figure 11). Solution can relatively quickly reach the core of the sample and, once there, can impinge the tablets from their lateral sides. Tablets can convert to HA in the sample core where they are locked into the structure. Conversion from the tablet exterior inward may create *c*-axis-elongated nanocrystallites (Figure 6) that, with prolonged dissolution–recrystallization, elongate with time and contribute to the increasing perpendicular orientation of the bulk (Table 2). In addition, degradation of the organic matrix that vertically separates each tablet followed by solution flow to these regions may induce conversion proceeding from the top and bottom of each tablet inward to produce bilayers of nanocrystallites with the parallel orientation (Figures 5c–f). However, this orientation is possibly the high energy product and may require higher temperatures and pressures to be expressed; at 140 °C, 4 bar, only the perpendicular orientation is observed with no bilayer tablets or parallel orientation apparent (Table 2).

The exterior surface of HA-converted nacre is randomly oriented with no morphology preservation because this region has had more prolonged exposure to hydrothermal conditions and its organic matrix is more degraded. Consequently, powder is released from the samples at this location.

Because the mineral phase of gastropod nacre has been shown to be continuous through the bulk, through myriad “mineral bridges” ($\sim 97/\mu\text{m}^2$) that connect the tablets in a stack and contribute to their high *c*-axis alignment,^{19,23} the possibility of topotaxy to the perpendicular orientation was investigated by crystal structure comparisons (described in the Experimental Section). In the crystal structure of aragonite, a pseudohexagonal unit cell with its *ab*-plane parallel to the orthorhombic *c*-axis was located in only the (010) plane with $a = b =$

9.94 Å, $c = 7.97$ Å, $\gamma = 120.07^\circ$, and a and b 2.53° out-of-plane from each other. In comparison with HA, this unit cell is 5.3% larger in a and contains two more Ca^{2+} and four more anions. Moreover, in the c -axis projection, the atomic positions in this cell are so different from those in HA that an anion exchange with preservation of crystallographic orientation is highly unlikely. Furthermore, no other pseudo-hexagonal cells with ab -planes parallel to the orthorhombic c -axis of aragonite were found that were as closely hexagonal ($a \neq b$; $|\gamma - 120| > 3^\circ$).

The possibility of topotaxy is seen less likely also by plan-view images of HA-converted tablets, as shown in Figure 6. Here, the long axes of HA nanocrystallites are oriented approximately radially about the tablet periphery. With solid-state topotaxy, these long axes would have a single orientation through the converted tablet because the original tablet was a single crystal. Instead, the changing long-axis directions of the nanocrystallites support flux-directed dissolution–recrystallization.

Comparison with biominerals that retain their form during HA conversion supports the importance of an interconnected organic network with an indirect vertical route through the material. For example, bivalve prismatic calcite has vertically straight organic spacers between distinct, regular prisms (Figure 7c)⁵² and converts only to HA powder. The long-needle morphology of the powder (Figure 7d) suggests that conversion was flux-directed, with the crystal growth axis projecting unimpeded through the prisms. Native eggshell and gastropod prismatic calcite have a more irregular, interconnected distribution of organic and, consequently, convert to HA with preservation of sample form.

Conclusion

Gastropod nacre (*Haliotis rufescens*) converts hydrothermally to HA with preservation of sample form, preservation of its tablet and stacks-of-tablets ultra-

structure, and a new unexpected orientation. This orientation, in which the c -axes of HA nanocrystallites are normal to the c -axis of the original aragonite, increases with reaction time and suggests that the aragonite–HA conversion occurs via dissolution–recrystallization rather than by solid state topotaxy. This orientation may be caused by the flux direction of the reaction solution through the nacre, which can follow the organic matrix in a zigzagging vertical path between stacks of tablets. Bivalve and cephalopod nacre disintegrate to HA powder by this reaction, possibly because they lack such a path. HA conversion is accompanied by thermal degradation of the organic and a corresponding decrease in hardness. The HA predominantly contains type A CO_3^{2-} , which substitutes at OH^- sites in the crystal lattice.

Acknowledgment. We thank Angela Belcher, Deron Walters, Fred Lange, Sarah Tolbert, Kirk Fields, and Ted Gier for technical support and discussions, Anna Davis and Aimee Rose for help with sample preparation and characterization, Aileen Morse and Deborah Gochfeld for coral, William Wise and Mike Jurashius for geological aragonite, and Steven Weiner for the *Atrina* shell. This paper was funded in part by a grant from the National Sea Grant College Program, National Oceanic and Atmospheric Administration, U.S. Department of Commerce, under grant number NA66RG0477, project number R/MP-82 through the California Sea Grant College System, and in part by the California State Resources Agency. The views expressed herein are those of the authors and do not necessarily reflect the views of NOAA or any of its subagencies. This work was also supported by grants from the Biosciences and Materials Research divisions of the National Science Foundation (DMR-9634396), the U.S. Army Research Office Multidisciplinary University Research Initiative (DAAH04-96-1-0443), and the U.S. Office of Naval Research (N00014-93-1-0584). This work made use of MRL Central Facilities supported by the National Science Foundation (DMR-9123048).

CM970785G

(52) Nakahara, H.; Kakei, M.; Bevelander, G. *Venus* **1980**, 39, 167.